^{35}Cl NQR Relaxation in Chloral Cyclohexylhemiacetal *

Haruo Niki and Ryokan Igei

Department of Physics, Division of General Education, University of the Ryukyus, Nishihara, Okinawa 903-01, Japan

Hiroshi Kyan and Takeshi Hamagawa

Department of Physics, College of Science, University of the Ryukyus, Nishihara, Okinawa 903-01, Japan

Takahiro Isono and Masao Hashimoto

Department of Chemistry, Faculty of Science, Kobe University, Nadaku, Kobe 657, Japan

Z. Naturforsch. **47a**, 299–304 (1992); received July 25, 1991

The crystal structure of cyclohexylhemiacetal (cycHx-CH) was determined at 296 K: monoclinic, space group $P2_1/c$, $a=1028.7(9)$, $b=609.5(1)$, $c=1811.9(4)$ pm, and $\beta=99.79(3)°$, $Z=4$, $R=0.0552$. The three ^{35}Cl NQR lines in cycHx-CH, T_1, T_2, and T_2^*, were measured by a pulsed method at 80–300 K. Below 200 K T_1^{-1} obeyed the T^2 law well, indicating that the spin lattice relaxation is governed by lattice vibrations. The reorientation of CCl_3 seems to be responsible for the sharp T_1 drop observed above 250 K. Shoulders in the T_1 vs. $1/T$ curves indicate the presence of T_1 minima at about 240 K. A fluctuation of the EFG due to a dynamic disorder of hydrogen atoms in the OH groups is assumed to explain the T_1 minima.

Key words: Chlorine NQR, Spin-lattice relaxation, Hydrogen bond, Crystal structure.

Introduction

In the previous work it was found that the spin lattice relaxation time (T_1) of Cl NQR of chloral n-butylhemiacetal (nB-CH) shows an unusual minimum at around 240 K [1]. This behavior has been tentatively explained by the fluctuation of the electric field gradient (EFG) caused by a dynamic disorder of hydrogen atoms in the hydrogen bond chains of the compound. Moreover, a peculiar minimum of the spin-spin relaxation time (T_2) was also found for nB-CH and chloral iso-butylhemiacetal (isoB-CH) [2].

The title compound, chloral cyclohexylhemiacetal (cycHx-CH), as well as nB-CH and isoB-CH are members of homologues having the formula $CCl_3CH(OH)OR$. In the present work we investigated the relaxation times of Cl NQR and the crystal structure of cycHx-CH to study the molecular motions in the crystal.

* Presented at the XIth International Symposium on Nuclear Quadrupole Resonance Spectroscopy, London, United Kingdom, July 15–19, 1991.

Reprint requests to Dr. Haruo Niki, Department of Physics, Division of General Education, University of the Ryukyus, Nishihara, Okinawa 903-01, Japan.

Experimental

Preparation of cycHx-CH

The compound was prepared as described in [3] and purified by recrystallizations from petroleum ether.

^{35}Cl NQR

T_1, T_2 and the inverse line width parameter (T_2^*) of ^{35}Cl NQR were measured with a conventional pulse spectrometer. T_1 was determined by the echo sequences $90°-\tau-90°-\tau'-180°$ in the temperature range where the values of T_1 are longer than those of T_2, and by $90°-\tau-90°$ pulse sequences in the higher temperature range. T_2 was measured by a conventional spin echo method ($90°-\tau-180°$). T_2^* was determined as the time required for a given induction signal to decay to $1/e$ of its maximum value. Experimental values of T_2^* were directly obtained from the free induction tails following pulses and also from the shapes of individual echoes. The width of the 90° pulse was about 10 μs for ν_3 and about 20 μs for ν_1 and ν_2, since ν_1 is close to ν_2 (see below).

0932-0784 / 92 / 0100-0299 $ 01.30/0. – Please order a reprint rather than making your own copy.

Crystal Structure Analysis

The crystal structure of cycHx-CH was determined by the single crystal technique at room temperature using Mo Kα radiation. The experimental details are given in Table 1. The crystal structures were solved by the direct method (MULTAN 78) [4] and refined by the least-squares method (HBLS-V) [5]. For two hydrogen atoms (H7 and H12), their positions and the temperature factors were not refined, but fixed. All calculations were performed on an ACOS 1000 Computer at the Information Processing Center of Kobe University with the UNICS system [6].

Infrared Spectrum and Dielectric Measurements

Infrared (IR) spectra were recorded on a Hitachi EPI-G2 spectrometer. The temperature dependence of the spectra was measured by using a conventional cryostat described in [7].

The dielectric losses were measured by means of an LCR meter (ANDO, AG-4311). The frequency range used was 0.1 to 100 kHz.

Table 1. Experimental conditions for the crystal structure determination and crystallographic data of chloral cyclohexylhemiacetal.

Formula	$C_8H_{13}Cl_3O_2$
Molecular mass, g/mol	247.5
Crystal habitus	needle
Size/mm^3	$0.4 \times 0.4 \times 0.3$
Diffractometer	Rigaku AFC-5
Wavelength, λ/pm	71.073 (Mo Kα)
$(\sin\theta/\lambda)_{max}$/pm^{-1}	0.00594
Monochromator	graphite
Temperature, T/K	296
Linear absorption coefficient, μ/m^{-1}	790
Lattice constants a/pm	1028.7(9)
b/pm	609.5(1)
c/pm	1811.9(4)
β/°	99.79(3)
Volume of the unit cell $V \cdot 10^{-6}$/pm^3	1119.4(10)
Space group	C_{2h}^5-P2$_1$/c
Formula units/unit cell	$Z=4$
d_{calc}/(Mg · m^{-3})	1.469
d_{obs}/(Mg · m^{-3})	1.483
Scan	$2\theta-\omega$
Number of measured reflections	2200
Symmetry independent reflections	1112
Reflections considered	847
Number of free parameters	163
$F(000)$	512
$R(F)$	0.0552
$R_w(F)$	0.0736

Point positions. All atoms in 4e:

x, y, z; $\bar{x}, \frac{1}{2}+y, \frac{1}{2}-z$

$\bar{x}, \bar{y}, \bar{z}$; $x, \frac{1}{2}-y, \frac{1}{2}+z$

Results

Crystal Structure of cycHx-CH

Table 1 gives the crystallographic data of cycHx-CH. Table 2 lists the positional and thermal parameters of the atoms in the asymmetric unit of the crystal. The bond lengths and bond angles are given in Figs. 1 and 2, respectively. The values given in these figures show no unusual features. The molecular packing projected along the b axis onto the (ac) plane is shown in Figure 3.

^{35}Cl NQR

Figure 4 shows the temperature dependence of the ^{35}Cl NQR frequencies (ν_1, ν_2, and ν_3). Since three lines are close to each other, the measurements of relaxation times of Cl NQR by the pulsed method were carefully carried out at all temperatures investigated.

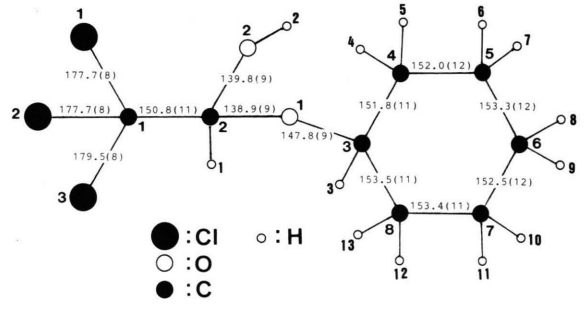

Fig. 1. Bond lengths (in pm) in a chloral cyclohexylhemiacetal (cycHx-CH) molecule. The bond lengths involving hydrogen atoms are not given.

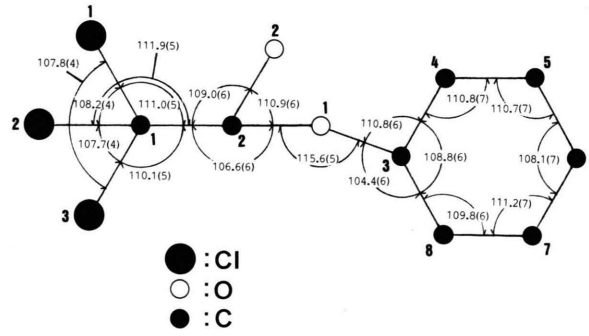

Fig. 2. Bond angles (in angular degrees) in cycHx-CH. The hydrogen atoms are not shown.

Table 2. Positional and thermal parameters (with standard deviations) of chloral cyclohexylhemiacetal. The temperature factor exponent has the form: $-(B_{11}\cdot h^2+B_{22}\cdot k^2+B_{33}\cdot l^2+B_{12}\cdot hk+B_{13}\cdot hl+B_{23}\cdot kl)$ for non-hydrogen atoms, $-B_{iso}\sin^2\theta/\lambda^2$ for hydrogen atoms. The temperature factors (B_{nm}) are given in units of $(10^{-10}\ \mathrm{m})^2$.

Atom	x/a	y/b	z/c	B_{11} or B_{iso}	B_{22}	B_{33}	B_{12}	B_{13}	B_{23}
Cl1	0.0565(2)	0.7148(3)	0.4361(1)	0.0141(3)	0.0338(5)	0.0036(1)	0.0022(6)	0.0060(4)	−0.0033(3)
Cl2	0.1262(2)	0.2723(2)	0.4032(1)	0.0165(3)	0.0232(4)	0.0034(1)	−0.0004(6)	0.0025(4)	0.0042(3)
Cl3	0.3231(2)	0.6139(4)	0.4177(1)	0.0092(2)	0.0527(7)	0.0044(1)	−0.0099(7)	0.0010(4)	−0.0041(5)
O1	0.1937(5)	0.4627(5)	0.2655(3)	0.0133(6)	0.0177(9)	0.0036(3)	0.0072(13)	0.0067(9)	0.0024(8)
O2	−0.0161(5)	0.5672(6)	0.2774(3)	0.0101(6)	0.0246(11)	0.0039(3)	0.0010(14)	0.0025(9)	0.0006(9)
C1	0.1526(6)	0.5533(9)	0.3840(4)	0.0091(8)	0.0216(14)	0.0035(4)	−0.0048(17)	0.0038(12)	−0.0020(11)
C2	0.1186(6)	0.6037(7)	0.3015(4)	0.0096(8)	0.0166(13)	0.0026(3)	−0.0005(17)	0.0026(11)	0.0006(10)
C3	0.2296(6)	0.5464(8)	0.1951(4)	0.0109(8)	0.0180(12)	0.0033(4)	0.0004(17)	0.0063(11)	−0.0013(11)
C4	0.3334(7)	0.7253(9)	0.2111(5)	0.0115(9)	0.0242(16)	0.0034(4)	−0.0058(20)	0.0045(13)	−0.0026(12)
C5	0.3825(9)	0.7924(9)	0.1399(5)	0.0171(12)	0.0243(17)	0.0040(4)	0.0023(23)	0.0077(15)	0.0021(13)
C6	0.4442(8)	0.5962(10)	0.1057(5)	0.0131(10)	0.0276(18)	0.0042(4)	0.0006(22)	0.0060(14)	0.0024(14)
C7	0.3400(8)	0.4166(10)	0.0897(5)	0.0133(10)	0.0313(18)	0.0033(4)	0.0031(23)	0.0039(14)	−0.0054(14)
C8	0.2902(7)	0.3478(9)	0.1614(4)	0.0092(8)	0.0190(13)	0.0031(4)	0.0007(18)	0.0017(12)	−0.0016(12)
H1	0.1420(56)	0.7786(72)	0.2939(36)	0.3					
H2	−0.0619(113)	0.6990(162)	0.2583(60)	7.7					
H3	0.1575(97)	0.6104(128)	0.1673(55)	5.7					
H4	0.4168(56)	0.6883(77)	0.2530(33)	0.3					
H5	0.2988(91)	0.8543(132)	0.2364(49)	5.0					
H6	0.4437(80)	0.9079(109)	0.1488(47)	3.9					
H7	0.2994	0.8537	0.0995	3.0					
H8	0.5208(71)	0.5437(100)	0.1397(42)	2.8					
H9	0.4626(73)	0.6547(108)	0.0528(43)	3.3					
H10	0.3725(69)	0.2971(94)	0.0700(42)	2.3					
H11	0.2710(86)	0.4654(137)	0.0524(50)	6.2					
H12	0.3692	0.2919	0.2030	2.0					
H13	0.2387(57)	0.2281(68)	0.1578(36)	0.4					

The temperature dependence of T_1 and T_2 of the Cl NQR are shown in Figure 5. The three resonance lines faded out at about 300 K. In addition to the sharp drop of T_1 appearing above about 180 K, each of the T_1 vs. $1/T$ curves shows a shoulder at around 240 K. This phenomenon indicated the presence of T_1 minima superimposed on the sharp drop of T_1.

The values of T_2^* for ν_1, ν_2, and ν_3 were in the range between 40 μs and 130 μs, indicating that lattice imperfections dominate the widths of the NQR lines.

IR spectrum and dielectric behavior

The IR band assigned to the OH stretching vibration was found to split into two components (3457 and 3409 cm^{-1} at ca. 289 K and 3437 and 3371 cm^{-1} at ca. 82 K). The relative intensity of the lower wavenumber component became markedly stronger at lower temperatures, as shown in Fig. 6. The OD stretching band in the deuterated compound exhibited the same feature. No appreciable dielectric loss was detected in the temperature range between 150 K and 300 K under the applied frequency range between 0.1 kHz and 100 kHz.

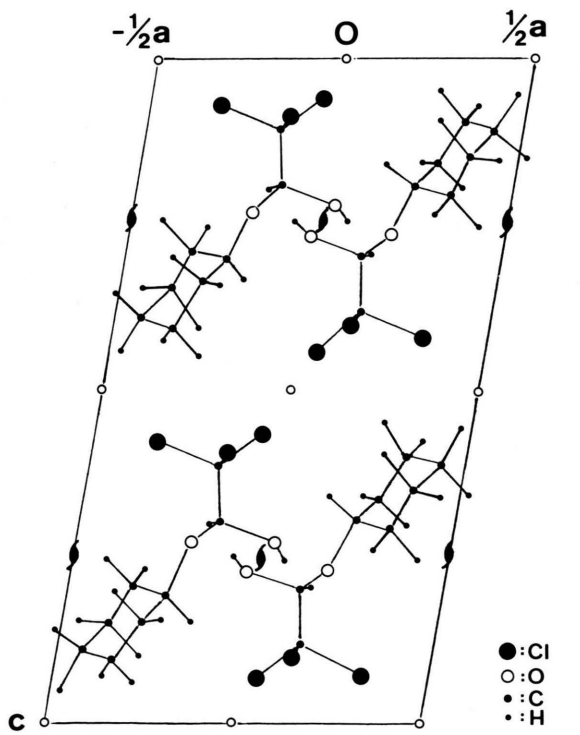

Fig. 3. The crystal structure of cycHx-CH projected along the *b*-axis onto the (*ac*) plane.

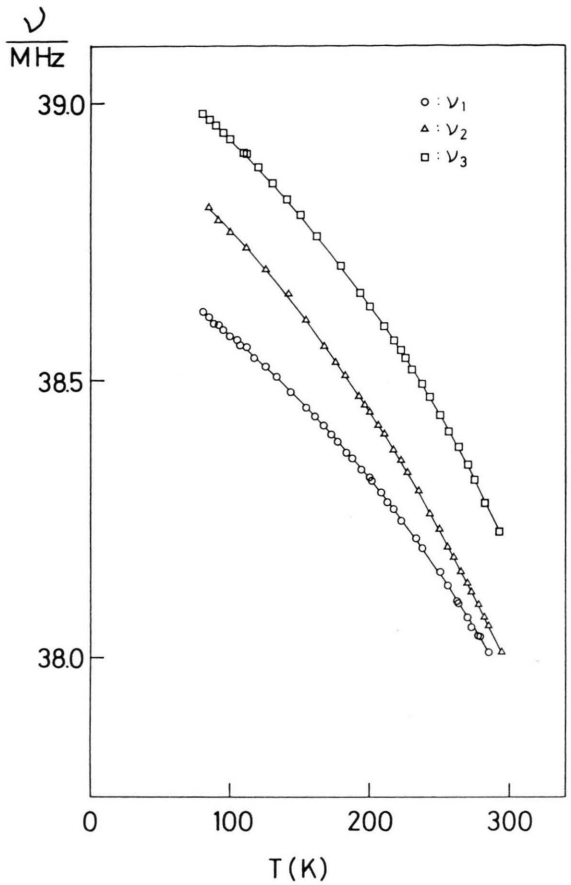

Fig. 4. Temperature dependence of the resonance frequencies of ^{35}Cl NQR in cycHx-CH.

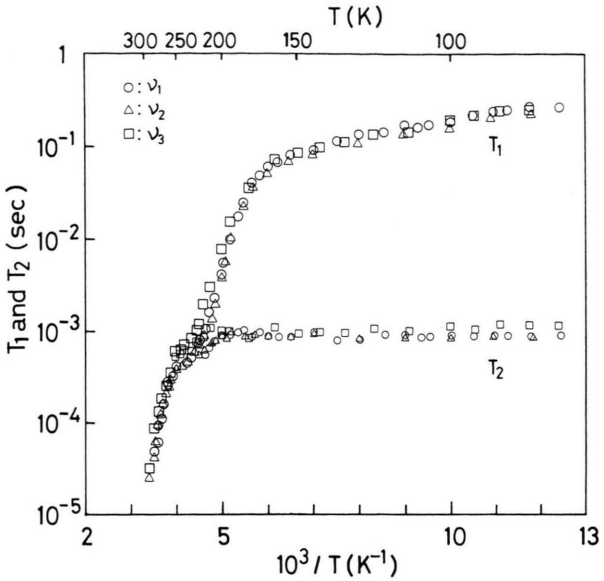

Fig. 5. Temperature dependence of T_1 and T_2 of ^{35}Cl NQR in cycHx-CH.

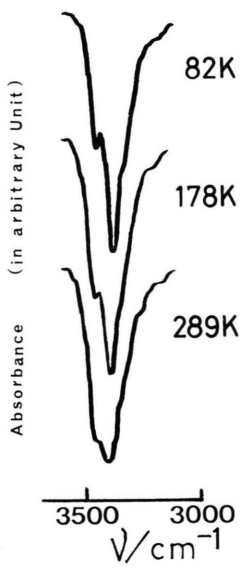

Fig. 6. Infrared absorption band assigned to the OH stretching vibration in cycHx-CH at various temperatures.

Discussion

The T_1 behavior below 200 K can be interpreted by the T^2 law [8]

$$T_1^{-1} = a T^2, \tag{1}$$

where a is constant. The values of $10^3 a$ are 0.54 ± 0.01 for ν_1, 0.60 ± 0.01 for ν_2 and 0.52 ± 0.01 for ν_3.

For convenience, the T_1 behavior above 250 K will be discussed next. The T_1 vs. $1/T$ curves in this temperature range can be described by the equation

$$T_1^{-1} = b \exp(-E_a/RT). \tag{2}$$

The values of $10^{-12} b$ and E_a for three lines are 3.48 ± 0.14 and 45 ± 5 kJ/mol, respectively. The magnitude of E_a of about 45 kJ/mol is comparable to those found for CCl_3 groups in a number of compounds [9]. Therefore, the T_1 behavior of cycHx-CH above ca. 250 K can be explained by the reorientation of the CCl_3. It should be noted, however, that this explanation is an approximate one, and, if the T_1 behavior shown in Fig. 6 is examined closely, a break in the T_1 vs. $1/T$ curve seems to exist at about 280 K. A detailed study on this point is now in progress.

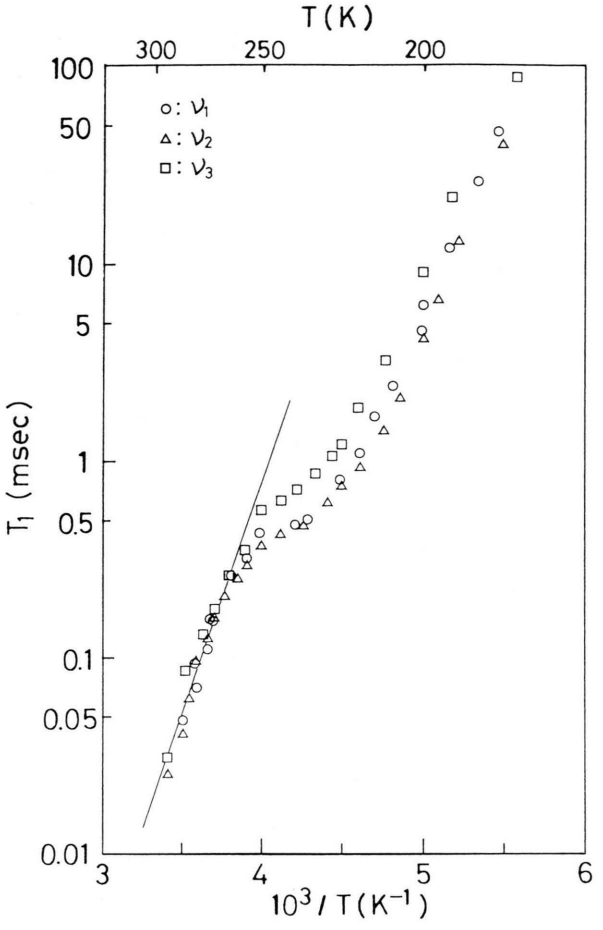

Fig. 7. Temperature dependence of T_1 obtained by subtracting the T_1^{-1} calculated by (1) from the observed values. The solid line denotes the values of T_1 calculated by (2) with $E_a = 45$ kJ/mol.

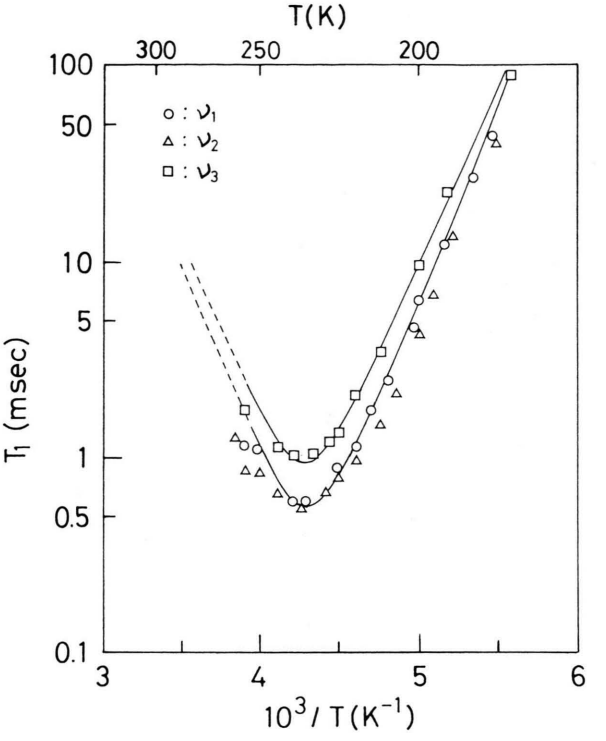

Fig. 8. Temperature dependence of T_1 obtained by subtracting the T_1^{-1} expressed by (1) and (2) from the observed values. The solid and broken curves are calculated by (3).

In the temperature range from 180 K to 280 K the T_1 vs. $1/T$ curves are anomalous: they have shoulders at about 240 K. In order to examine the T_1 behavior around 240 K in detail, the parts of the spin-lattice relaxation rate given by (1) were subtracted from the observed values of T_1^{-1}. The results shown in Fig. 7 indicate the presence of T_1 minima superimposed on the sharp decrease of T_1 due to the motion of the CCl_3 group. Then, T_1 vs. $1/T$ curves with T_1 minima shown in Fig. 8 were extracted as differences between the T_1 shown in Fig. 7 and those calculated by using (2). The T_1's can be described approximately by the equation * [8]

$$\frac{1}{T_1} = \frac{C\tau}{1+(\omega\tau)^2}, \qquad (3)$$

where $\tau = \tau_0 \exp(E_m/RT)$. The values of $10^{17}\tau_0$ are 2.52 s for ν_1 and ν_2 and 8.93 s for ν_3. The values of E_m are 36.7 ± 3.0 kJ/mol for ν_1 and ν_2, and 34.3 ± 3.0 kJ/mol for ν_3. The solid and broken curves in Fig. 8 denote the values of T_1 calculated by (3) with τ_0 and E_m as obtained above.

The spin-lattice relaxation due to the electric quadrupole interaction is far more important than that due to the magnetic dipole-dipole interaction. Therefore we consider only the electric contribution to T_1 arising from a particular lattice motion. For the unusual T_1 minimum (<0.01 ms) found for nB-CH, a jumping motion of hydrogen atoms in the OH groups associated with a dynamic disorder has been proposed as a possible source of the fluctuation of EFG. The crystal structure of cycHx-CH is quite similar to that of nB-CH; both crystals are characterized by chains of O–H ··· O hydrogen bonds running along a 2_1 axis. It seems probable that similar dynamic disorder to that of nB-CH takes place in cycHx-CH, too. The

* An equivalent potential well for the hydrogen atoms is assumed here.

splitting of the IR OH band found for cycHx-CH supports this idea. Therefore, one may assume the same mechanism as in nB-CH to interpret the T_1 minimum observed with cycHx-CH.

According to this mechanism, it is reasonable that the value of the T_1 minimum of ν_3 differs from those of ν_1 and ν_2 because the distance between the corresponding Cl atom and the fluctuating H atom is different. The observation that appreciable dielectric dispersion could not be detected might indicate that the magnitude of the fluctuation of the hydrogen atoms is too small to produce significant dielectric dispersion.

[1] M. Hashimoto, T. Isono, H. Niki, and T. Higa, Z. Naturforsch. **45a,** 472 (1990).
[2] H. Niki, R. Igei, T. Higa, M. Hashimoto, and T. Isono, Z. Naturforsch. **45a,** 481 (1990).
[3] Beilstein, Band I, S. 619.
[4] P. Main, S. E. Hull, L. Lessinger, G. Germain, J. P. Declercq, and M. M. Woolfson, MULTAN 78, a System of Computer Programs for the Automatic Solution of Crystal Structures from X-ray Diffraction Data. Universities of York, England, and Louvain, Belgium 1978.
[5] T. Ashida, The Universal Crystallographic Computing Systems – Osaka, HBLS-V, p. 53. The Computer Center, Osaka University, Japan.
[6] T. Sakurai and K. Kobayashi, Rikagaku Kenkyusho Hokoku **55,** 69 (1979).
[7] Y. Mido and M. Hashimoto, J. Mol. Struct. **129,** 253 (1985).
[8] D. E. Woessner and H. S. Gutowsky, J. Chem. Phys. **39,** 440 (1963).
[9] H. Chihara and N. Nakamura, Advances in Nuclear Quadrupole Resonance (J. A. S. Smith, ed.) **4,** 1, Heyden, London 1980.